Materials Advances

Accepted Manuscript

This article can be cited before page numbers have been issued, to do this please use: S. Ponnada, D. B. Gorle, M. S. Kiai, R. Saravanakumar, R. K. Sharma and A. Nowduri, *Mater. Adv.*, 2021, DOI: 10.1039/D1MA00319D.

View Article Online
DOI: 10.1039/D1MA00319D

Facile Cost-Effective Rapid Single-Step Synthesis of Ag-Cu Decorated ZnO Nanoflower like composites (NFLC) for Electrochemical Sensing of Dopamine

Srikanth Ponnada[a]*, Demudu Babu Gorle[b], Maryam Sadat Kiai[c]*, Saravanakumar Rajagopal[d], Rakesh Kumar Sharma[e], Annapurna Nowduri[a]*

[a]*Department of Engineering Chemistry, Andhra University College of Engineering (A), Andhra University, Visakhapatnam-530003, India.*

[b]*Materials Research Centre, Indian Institute of Science, Bengaluru-560012, India.*

[c]*Nano-Science and Nano-Engineering Program, Graduate School of Science, Engineering and Technology, Istanbul Technical University, Istanbul-34469, Turkey.*

[d]*Department of Chemistry, Thiagarajar College of Engineering, Madurai, Tamil Nadu-625005, India.*

[e]*Sustainable Materials and Catalysis Research Laboratory (SMCRL), Department of Chemistry, Indian Institute of Technology Jodhpur, Karwad, Jodhpur-342037, India.*

Corresponding Author's

1. **Dr. Annapurna Nowduri**
   [a]***Email**- dr.nannapurna@andhrauniversity.edu.in

2. **Maryam Sadat Kiai**
   [b]***Email**- maryamskiai@gmail.com

3. **Srikanth Ponnada**
   [a]***Email**- koolsreekanth@gmail.com

View Article Online
DOI: 10.1039/D1MA00319D

Abstract

For clinical biology, the ability to detect neurotransmitters in human serum environment quickly, highly sensitively, and selectively is essential. Dopamine system dysfunction has been linked to a variety of nervous system diseases. As a result, its sensitive and selective detection is critical for the early diagnosis of diseases associated with excessive dopamine levels. So, platforms for sensitive and selective monitoring of dopamine concentrations are critically needed.

In this study, we synthesized a facile flower-like nanocomposite material that is cost effective and involves a rapid single-step synthesis of Ag-Cu decorated ZnO nanoflower like composite (Ag-Cu@ZnO-NFLC) with a high active surface area for comparison. Ag decorated ZnO (Ag@ZnO) and Cu decorated ZnO (Cu@ZnO) were synthesized and characterized by XRD, FTIR, Raman, Using methods such as cyclic voltammetry, differential pulse voltammetry (DPV), and amperometry, the electrochemical behavior of GCE modified with single step synthesized Ag-Cu decorated ZnO nano flower like composite electrode material showed promising results with an ultra-low detection limit of 0.21 μM, high sensitivity of 0.68 $\mu AmM^{-1}cm^{-2}$ and by employing Differential pulse voltammetry (DPV). The dopamine sensor was also tested for current density at different pH levels, and it demonstrated good stability and reproducibility. Finally, the prepared sensor was used to monitor real-time human urine samples, yielding excellent results. The findings revealed that in actual sample analyzing, the as-prepared sensor had substantial promising results in detecting the dopamine.

Keywords: Ag-Cu decorated ZnO nanoflower like composite, hydrothermal method, electrochemical sensor, Dopamine, Cyclic Voltammetry, Amperometry.

View Article Online
DOI: 10.1039/D1MA00319D

1. Introduction

Dopamine (DA) is a neurotransmitter that belongs to the family catecholamine and phenethylamine, usually found in the nervous system **Fig.S3**. Kidneys and cardiovascular systems of mammals [1]. Lower or abnormal concentrations of dopamine in the blood leads to malfunctioning of kidneys, heart and serious diseases like Parkinson's, schizophrenia etc. Hence, there is a severe necessity for detecting dopamine concentrations in diagnostic practices [2]. Till date, several research groups have reported many strategies and employed different techniques to detect dopamine such as chromatography, capillary electrophoresis [3] and surface-enhanced raman scattering method [4] and high-performance liquid chromatography (HPLC) [5]. All of these methods require a standard experimental setup and are not cost effective. However, in order to overcome these limitations, electrochemical detection [6] and synthesis of nanomaterials [45] has emerged and been reported by various research groups due to its low cost, simple experimental setup, sensitivity, and a wide range of materials available for modifying the electrode surface; typically, a glassy carbon electrode is used and the surface is modified by nanomaterial's like metal oxide composites including Au [7], CuO [8], Ag [9], ZnO [10] Metal organic frame works (MOF) [11] etc. are widely employed because of their high electron mobility, morphological variety, and ease of synthesis.

ZnO has been in the spotlight for a decade due to its promising catalytic activity, cost effectiveness, high surface area, nontoxicity, and bio affinity. As a result, ZnO-based nanomaterials are being used extensively in recent developments to fabricate electrochemical sensors. Cu doped single phase ZnO plates synthesized via hydrothermal method and have been employed for electrochemical detection of dopamine showed promising performance [12] The ionic medium

View Article Online
DOI: 10.1039/D1MA00319D

supported reduced graphene oxide (im-rGO) has been reported for electrochemical sensing of dopamine [13], DNA electrochemical sensing via Ag nanoparticles decorated on carbon nanocubes has been reported for electrochemical sensing of H_2O_2 [14], Ag@ZIF-67/GCE has been reported for electrochemical sensing of H_2O_2 [15], Nanoparticles (NP 'S) of metals have been identified as potential candidates in bio sensing. Ag nanoparticles are employed in electrochemical detection because of their low oxidation potential [16]. Cu, on the other hand, is studied extensively for various applications like selective oxidation [17], photo catalysis [18], electrochemical sensing [18], [19], coming to ZnO due to great electron mobility and wide band gap, it is employed in electrochemical sensing [18], [19], [20]. Xuan Zhang et al. used GCE modified with reduced graphene oxide/ZnO nano composite and reported that the presence of ZnO in rGO showed an enhanced active surface area due to the versatile nature of ZnO, which in turn enabled the high sensing activity towards dopamine, uric acid, and ascorbic acid [21].

By using a chiral ligand such as L-cysteine, chiral ZnO nanoparticles were prepared and the average particle size ranged from about 4.5 ± 1.1 nm. These chiral ZnO nanoparticles exhibited promising electrochemical behavior [22].

The interference of ascorbic acid and uric acid was suppressed during the detection of dopamine when the novel porous rGO encapsulated ZnO microspheres were employed as surface modifiers for glassy carbon, which is a working electrode. The P-rGO acted as a Schottky barrier by suppressing the interference of AA and UA [25]. Azam Anaraki Firooz et al. reported Cu doped ZnO nanostructures modified with GCE showed excellent electrochemical activity towards dopamine sensing [26]. Cu is reported to be an excellent catalytic material with high tunability and stability. In other experiments, Au nanoparticles-ZnO were used, which required precious high-cost Au and a longer synthesis time [27], or ZnO sensor synthesis using microwave aided synthesis

View Article Online
DOI: 10.1039/D1MA00319D

[29]. The dropping technique was used by Xiaowei et al. to test the carbon/ZnO microfibers' Dopamine (DA) sensing ability. With a detection limit of 0.106 M, the suggested sensor demonstrated high selectivity, repeatability, and stability. Carbon/ZnO-GCE demonstrated reduced over-potential, reduced potential difference, and increased peak currents at 0.191/0.238 V, demonstrating the improved catalytic actions of carbon/ZnO microfibers toward DA [28]. Because hollow carbon spheres have been shown to have high surface area and great mass mobility properties, and Ag particles have been shown to have great bio-affinity, high electron mobility, and prominent catalytic reaction. Recently, Xinjin Zhang et al. synthesized Ag nanoparticles decorated mesoporous hollow carbon spheres. As a result, the synthesized Ag-HCS/GCE showed a wide linear range and high sensitivity [30]. Recently, for the ultrasensitive detection of dopamine (DA), an electrochemical sensor based on Ag nanoparticles anchored onto CuO porous nanobelts (Ag/CuO PNBs) was developed by Gang Liu et al. DA was produced by a simple two-step cation-exchange procedure followed by in-situ thermal conversion. The anchoring Ag NPs have a large catalytic role in the redox process, and the Ag/CuO PNBs are porous structures with more active sites [31].

Table-1 depicts the comparisons of different ZnO based nanomaterials in electrochemical sensing of dopamine. To take advantage of both Ag and Cu metals due to their proven properties such as bio-affinity and selectivity towards dopamine and high electron mobility and low band gap nature of ZnO, in this work, we synthesized a single step. This method suggested a cost effective facile Ag-Cu decorated ZnO nanoflower like composite (NFLC) material which involved a rapid hydrothermal synthesis.

The resultant sensor exhibited high sensitivity and selectivity towards the detection of dopamine at room temperature without any further interference.

View Article Online
DOI: 10.1039/D1MA00319D

2. Experimental Section

2. 1. Materials and chemicals used

Copper nitrate ($Cu(NO_3)_2$), silver nitrate ($AgNO_3$), zinc nitrate ($Zn(NO_3)_2$) and ammonium hydroxide (NH_4OH) were purchased from Sigma Aldrich, India. Ethanol, acetone, were procured from Himedia Laboratory Pvt. Ltd., Mumbai, India. Caffeic acid, uric acid, β-endorphin, ascorbic acid, histamine, trypramine, phenethylamine, serotonin and acetylcholine were purchased from Alfa-Aesar. All reagents and solvents were purchased from Sigma-Aldrich/Alfa Aesar and used without further purification.

2. 2. Synthesis of Ag-Cu Decorated ZnO nanoflower like composites (NFLC)

The Cu/ZnO nanocomposite was prepared in a single step hydrothermal method, in which an aqueous solution of 0.5 M zinc nitrate (Zn (NO_3) $2.6H_2O$) (Sigma Aldrich) and 0.05 M copper nitrate Cu $(NO3)_2$ (Sigma Aldrich) were mixed under constant stirring for about 1 hour at the ambient temperature. A pH value of 9.5 was maintained by gradually adding a few drops of ammonium hydroxide. The resultant solution was then transferred into a Teflon-lined autoclave followed by vigorous stirring for 30 min. Henceforth, the autoclave was sealed and heated up to 180 ºC for 6 h. And the final product was washed several times with ethanol and deionized water (DI) water and dried at 60 ºC in a hot air oven overnight, whereas Ag/ZnO nanocomposite was prepared through a single step hydrothermal method. The aqueous solution of 0.5 M zinc nitrate (Zn $(NO3)_2$ $.6H_2O$) (Sigma Aldrich) and 0.05 M silver nitrate ($AgNO_3$) (Sigma Aldrich) were mixed under constant stirring for 1 hour at the ambient temperature. The pH value of 9.5 was maintained by adding ammonium hydroxide into the solution drop by drop steadily. The resultant

View Article Online
DOI: 10.1039/D1MA00319D

solution was then transferred into a Teflon-lined autoclave and made to stir vigorously for 30 min. Henceforth, the autoclave was sealed and heated up to 180 ºC for 6 h. The final product was washed several times with ethanol and deionized water (DI) water and dried at 60 ºC in a hot air oven overnight.

The Ag-Cu decorated zinc oxide nanoflower like composite was made in a single step by mixing an aqueous solution of 0.5 M zinc nitrate (Zn (NO_3) $2.6H_2O$), 0.05 M silver nitrate (AgNO3), and 0.05 M copper nitrate Cu $(NO_3)_2$ for 1 hour at the room temperature. The pH value of 9.5 was maintained by adding a few drops of ammonium hydroxide into the solution drop by drop very slowly. The resultant solution was then transferred into a Teflon-lined autoclave followed by vigorous stirring for 30 min. After this, the autoclave was sealed and heated up to 180 ºC for 6 h. The final product was washed several times with ethanol and deionized water (DI) water and dried at 60 ºC in a hot air oven overnight. The XRD, XPS, FT-IR, Raman, EDAX and FE-SEM analysis were conducted to study the elemental composition and morphology of synthesized samples.

2. 3. Characterization and Electrochemical techniques

FT-IR analysis was carried out on a Bruker Tensor 27 (Optik GmbH) using the RT DLaTGS (Varian) detector. Powder X-ray diffraction (PXRD) patterns were recorded at room temperature (RT) using a RigaKu Smart lab guidance instrument using Copper (Rotating Anode) with an X-Ray Power of 200 ma, 45KV (9kW). Detector's scintillation counter (0D), D/tex(1D) HyPix-3000 (Hybrid Pixel Array Detector (2D)). The powder diffraction covered the angle ranges from 10−90°, with a step angle of 6°/min respectively. Raman spectra were recorded using a high-resolution Renishaw Raman microscope employing a He−Ne laser of 18 mW at 633 nm. The morphological

View Article Online
DOI: 10.1039/D1MA00319D

structures of the prepared samples were captured using a scanning electron microscope (SEM) of TESCAN, VEGA 3 with Bruker detector respectively. The high-resolution XPS spectra of the as-synthesized samples were recorded on a Theta Probe AR-XPS system. Cyclic voltammetry was carried out on a Biologic SP-150 workstation, at room temperature in a standard three-electrode cell and the working electrode was a Glassy carbon (GC) (area = 0.07 cm^2), modified glassy carbon and the counter electrode was a Pt wire. The reference electrode used was Ag/AgCl/KCl (3 M) electrode respectively.

2. 4. Electrochemical measurement

Fine alumina powder having a diameter of 0.05 and 0.3 μM was used to polish the surface of the glassy carbon electrode (GCE). The GCE was pre-treated before the surface modification, as per the procedure mentioned in the above section. Preceding to the fabrication of Ag-Cu@ZnO-NFLC modified GCE, the GCE was dried at room temperature and nitrogen gas was purged continuously for half an hour. Later, 10 μL of Ag@ZnO, Cu@ZnO and Ag-Cu@ZnO-NFLC were suspended in 100 μL of ethanol and sonicated for 20 min. By using the drop casting method, the subsequent blend of (3 μL) was drop casted onto the surface of GCE. And then the modified electrode was cleaned four times with DD water and ethanol to eliminate the unbound nanocomposite materials.

3. Results and Discussion

3. 1. Physical characterization of Ag-Cu decorated ZnO NFLC

The FTIR spectrum of Ag-Cu decorated ZnO composite was recorded in the range of 400-4000 cm^{-1}, and is shown in **Fig. 1A.** FTIR spectroscopy provides useful information about various functional groups and metal-oxide bonds present in the composite. A significant vibration band obtained at 509 cm^{-1} corresponds to the characteristic stretching mode of the Zn-O bond. Two

View Article Online
DOI: 10.1039/D1MA00319D

broad peaks at 3542 cm^{-1} (stretching) and 1280 cm^{-1} to 1470 cm^{-1} (bending) indicate the presence of an O-H functional group which is due to the absorption of atmospheric moisture on the surface of the composite [41-43]. To further confirm the components of the composite, Raman analysis was conducted and shown in **Fig. 1B.** Two peaks are detected at 60 cm^{-1}, and 254 cm^{-1} for Cu and Ag with enhancement in the intensity, which is considered as evidence for the formation of Ag-Cu alloy nanoparticles. The main E2 mode of ZnO is clearly visible along with the Raman peaks of Ag and Cu, confirming the presence of Ag-Cu and ZnO in the NFL composite. A weak intensity peak is detected at 430 cm^{-1} in ZnO particles. The low peak of ZnO may be because its surface area is decorated with Ag-Cu alloy, so the Raman peak intensity is relatively low. In XRD **Fig. 1C** shows the XRD spectrum of Ag-Cu@ZnO NFLC. The diffraction peaks observed at 2θ= 38.34, 44.31 and 64.65 are assigned as (111), (200) and (220) crystal planes, respectively, of the face-centred cubic phase of Ag. The peak positions match the PDF file for Ag (PDF: 01-089-3722). The diffraction peaks observed at 2θ= 43.51 and 51.57 are assigned as (111) and (200) crystal planes, respectively, of the face-centred cubic phase of Cu. The peak position matches the PDF file for Cu (PDF: 01-085-1326) [30]. However, the diffraction peaks observed at 2θ = 32.27, 34.10, 36.50, 46.40, 55.25, 62.12 and 77.72 correspond to the (100), (002), (101), (102), (110), (103) and (202) crystal planes respectively and hexagonal crystal geometry of ZnO (JCPSD card no. 01-007-2551) [44]. **Fig. 2 A.** represents the SEM images of the Ag-Cu decorated ZnO composite having a nanoflower-like morphological structure with different magnifications [32]. The Energy-dispersive X-ray spectrum (EDX) reveals the presence of Cu, Ag, Zn, and O elements in the stoichiometric ratio as tabulated in **Fig. 2B.**

The XPS analysis of the nanoparticles reveals the oxidation states of the metallic species. The structural composition of Ag-Cu decorated ZnO nanoflowers was further characterized by the XPS

View Article Online
DOI: 10.1039/D1MA00319D

technique. **Fig. S1** shows the XPS survey spectra of the Ag-Cu decorated ZnO nanoflowers, indicating the presence of constituted elements (Ag, O, Cu, and Zn). **Fig. 3A** shows that Ag3d5/2 (368.2 eV) and Ag3d3/2 (374.5 eV) peaks are associated with 0-valent Ag at 368 and 374 eV, respectively. Besides, the good symmetry of the peaks proves that the valance of Ag does not change after the formation of the alloy with Cu. The composite shows the core-level and shakeup satellite lines of Cu 2p, as shown in **Fig. 3B**. In the XPS spectra (Fig. 3B), two Cu peaks at binding energies of 934.1 and 951.3 eV were observed, which corresponded to Cu2p3/2 and Cu2p1/2, respectively, demonstrating the successful production of Cu nanoparticles The existence of CuO (934.8 and 951.8 eV) along with the satellite peaks at 941.5 eV and 944.3 eV indicated that copper on the surface region could be easily oxidized at room temperature [33-36].

Fig. 3C shows the high-resolution XPS spectra of Zn 2p. The two symmetric signal peaks are formed at 1029.3 eV and 1052.6 eV correspond to Zn 2p3/2 and Zn 2p1/2, respectively, and the energy interval between the peaks is ~23 eV. The above information confirms that Zn is completely oxidized and is in +2 valance state. **Fig. 3D.** Illustrates the high-resolution spectra of O 1s. The peak appeared at 532.7 eV corresponding to the presence of a Zn-O bond in the ZnO structure [46].

3. 2. Electrochemical performance of Ag@ZnO, Cu@ZnO and Ag-Cu@ZnO NFLC/GCE towards dopamine detection

The nanocomposite materials were drop casted onto GCE and electrochemical performance was investigated using the cyclic voltammetry (CV) technique. For comparison, bare GCE was also included in **Fig. 4a** shows the CV current responses of GCE, Ag@ZnO, Cu@ZnO and Ag-

View Article Online
DOI: 10.1039/D1MA00319D

Cu@ZnO-NFLC in 0.1M PBS (pH 7.0) containing 100 μM of DA at a scan rate of 50 mVs^{-1}. Whereas bare GCE, the GCE surface modified with Ag@ZnO and Cu@ZnO nanocomposite shows no crystal-clear electrochemical response to the oxidation of DA. However, the GCE modified with Ag-Cu@ZnO nanoflower like composite exhibited a strong apparently reversible peak that is one anodic peak at 0.24 V and one cathodic peak at 0.005 V with high peak currents. However, the exceptional increase in the redox peak currents on Ag-Cu@ZnO-NFLC/GCE with competently characterized redox couple of dopamine can be allocated, to its higher electrocatalytic activity when compared with GCE, Ag@ZnO, Cu@ZnO nanocomposite samples. Perhaps the enhanced electrocatalytic activity is due to its association with synergic action between Ag support and Cu NPs on the increased surface area of the ZnO electrode surface.

The anodic current at the Ag-Cu@ZnO-NFLC/GCE increased significantly and well-defined oxidation and reduction waves were recorded. In addition, the stronger oxidation response measured at the composite Ag-Cu@ZnO-NFLC/GCE electrode seems to imply that this material creates a favorable microenvironment for dopamine oxidation, which might be connected to the composite electrode's higher surface area and better electron transfer rate.

Apart from this, the Ag-Cu nanocomposite material provides enhanced support for the adsorption of DA and also helps in the mobility of the electrons between GCE and the analyte henceforth, enabling it to a remarkable increase in the electron transfer rate. The mechanism of electrochemical oxidation of dopamine on the Ag-Cu@ZnO-NFLC/GCE surface is depicted in **Scheme-1** by the exchange of two protons and two electrons between the DA and electrochemically oxidized molecules.

View Article Online
DOI: 10.1039/D1MA00319D

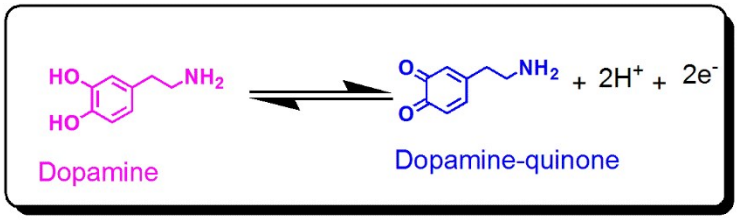

Scheme-1 Depicts Oxidation of Dopamine to Dopamine-quinone and its reduction to DA

When the dopamine hydrochloride is subjected to a ramping potential of -0.3 V to +0.5 V vs. Ag/AgCl, the transfer of electrons from the NFLC material to the GCE results in an increased faradaic current. Henceforth, optimization of pH value of 7.0 was identified from the CV current responses for 100 µM of DA on Ag-Cu@ZnO-NFLC/GCE in 0.1M PBS.

3.2.1. Studies on the effect of scan rate (sweep rate)

Fig. 4b. depicts the CV on the effect of various sweep rates ranging from 10 to 100 mV s^{-1} on the redox behavior of 100 µM DA at Ag-Cu@ZnO-NFLC/GCE in 0.1 M PBS (pH 7.0). The Ag-Cu@ZnO-NFLC/GCE has three well-resolved peaks (**Fig. 4b**). As shown in **Fig. 4b**, increasing the scan rate causes an increase in both the oxidation and reduction peaks currents, as well as a slight shift in the redox potential. The remarkable peak separation on Ag-Cu@ZnO-NFLC/GCE could be explained by its larger surface area, which facilitates electron transfer and increases adsorption strength toward biomolecules.

The plot of scan rate *vs* the peak current density exhibits that the linear regression equation for oxidation and reduction of peak currents is Ip_a (mA) = 0.03987 ν (mV/s) + 0.00024, R^2=0.99 Ipc (µA) = - 0.00391ν (mV/s) – 0.00031, R^2=0.98 respectively the **Fig. 4c.** depicts it and this linearity implies the role of surface-controlled process in its electrochemical kinetics. However, the

View Article Online
DOI: 10.1039/D1MA00319D

Randles-Sevick equation was used to calculate the diffusion coefficient of DA for bare GCE and Ag-Cu@ZnO/GCE using equation (1).

$$I_p = (2.69\times10^5)\, n^{3/2} A D^{1/2} C v^{1/2} \quad \text{---------- (1)}$$

Here, A is the electrode surface area, n is the number of electrons transferred, *v* is the scan rate, D is the diffusion co-efficient, I_p is the peak current and C is the concentration of DA from the above equation, calculated. The D values for Ag-Cu@ZnO/GCE and GCE were determined to be 7.496 $\times\ 10^{-6}$ $cm^2\ s^{-1}$ and 14.136 $\times\ 10^{-6}$ $cm^2\ s^{-1}$, respectively, and these improved D values may be correlated to the higher electrochemical active surface area for Ag-Cu@ZnO-NFLC modified GCE compared to bare GCE. Chronocoulometry (CC) is used to readily determine the real electrochemical active electrode area, as well as their respective diffusion coefficients, the time-window of an electrochemical cell and adsorption of electroactive species [37]. The result demonstrated a reversible reaction with the active area of 0.072 cm^2. As shown in **Fig. S2,** the optimized amount of the material drop coating on the electrode surface was determined as 1 mg/ml.

3.2.2. Studies with Amperometric i–t curve and Differential Pulse Voltammetry (DPV)

The DPV was performed in 0.1 M PBS for different concentrations of DA varying from 10 to 200 μM to study the oxidation and reduction behavior of DA at modified GCE depicted in **Fig. 5a**.

It could be emphasized that the changes in current are insignificant for different concentrations of DA varying from 10 to 200 μM, which indicates the stability of Ag-Cu@ZnO NFLC modified GCE composite modified electrode. Based on the result, it is obvious that the formed Ag-Cu on ZnO is highly stable and active and it is a suitable catalytic electrode for electrochemical redox reactions [40].

View Article Online
DOI: 10.1039/D1MA00319D

However, in order to formulate the mathematical relation between voltametric current response of Ag-Cu@ZnO-NFLC/GCE and DA concentration, a calibration curve has been established for the understanding curve depicted in **Fig. 5b.** The DPV studies clearly exhibited the I_p is linear with DA concentration with an enhanced high sensitivity of I (mA) =0.0291c (mA mM^{-1}) + 0.00033, (R^2=0.99) over a low limit of detection of 0.21 μM and a sensitivity of 0.68 μA $\mu M^{-1}cm^{-2}$.

3.2.3. Studies on Effect of pH in electrochemical response of DA on Ag-Cu@ZnO-NFLC/GCE Sensor

The studies of pH result in the electrochemical response of DA on Ag-Cu@ZnO nanoflower like composite modified GCE electrode over the pH starting from 4.0 to 9.0 in 0.1M PBS solution consisting of 100 μM of DA shown in **Fig. 5c.**

Fig. 5c. encapsulates that the oxidation peak current will increase with an increase in the solution pH from 4.0 to 9.0 and, henceforth, diminishes with a further increase in pH, illustrating the inclusion of protons within the electrode reaction processes, leading at maximum pH, a large amount of hydroxyl ions perhaps uproot DA on the surface assimilation sites of Au-Cu@ZnO nanoflower like composite surface. The DA exists in a non-dissociated kind once the pH of the solution is a smaller amount than pKa value (9.8), then it exists within the sort of associate ion at higher pH resulting in a lower current. Non-dissociated DA may be more adsorbate on the electrode surface than dissociated DA, resulting in the most extreme current response at a lower pKa value.

Since, electrochemical oxidation of DA includes deprotonation, electrode reaction diminishes at acidic conditions leading to a reduction of peak current. The pH of 7.0 is consistently chosen for the initial analytical experiments.

View Article Online
DOI: 10.1039/D1MA00319D

Fig. 6a. depicts the amperometric i-t responses recorded for different DA concentrations in the range of (0.1 μM – 10 μM) at Ag-Cu@ZnO-NFLC/GCE. An applied potential of 0.24 V was maintained between the Ag-Cu@ZnO-NFLC/GCE and the Ag/AgCl reference electrode in the amperometric i-t experiment, to 0.1 M PBS solution, and a continuous addition of 1 M of DA. It was spiked in order to record the current responses of the fabricated nanocomposite electrode. Simultaneously, the DA concentration was enhanced from 0.1 μM to 10 μM. The amperometric current response of fabricated nanocomposites electrode showed a rapid response to DA from the amperometric i-t curve. The response time for the rapid detection of DA is calculated as 3 seconds, which is one of the attributes of a DA sensor for the quick detection of DA in real time samples. Now **Fig. 6b.** represents the calibration curve established between amperometric current responses and various concentrations of DA in **Fig. 6b.** A linear plot with a high sensitivity of (I (mA) = 0.0475c mA μM^{-1}) + 0.00241, R^2=0.99) from 0.1 μM to 10 μM at low detection limit and higher sensitivity of 0.228 μM and 0.72 $\mu A \mu M^{-1} cm^{-2}$ respectively.

3.2.4. Studies on Stability, Interference and reproducibility studies of Ag-Cu@ZnO-NFLC/GCE Sensor

Amperometric current response for human urine sample was recorded to study the analytical capability of the proposed flower like nanocomposite modified GCE electrode. The collected human urine sample was added directly to the 0.1 M PBS pH 7.0 and an applied potential of 0.24 V was used between the fabricated working electrode and the Ag/AgCl reference electrode. **Fig. 6c.** showed an increased current response and it was observed when the urine sample was spiked with known concentrations of DA continuously at a regular interval of time that is 250 seconds.

View Article Online
DOI: 10.1039/D1MA00319D

Then the corresponding detected DA concentrations from amperometric current responses were 0.030 μM, 0.052 μM and 0.070 μM respectively from 1 μM of urine sample. All these results indicate that the fabricated nanocomposites electrode has the analytical capability to detect DA in human urine samples rapidly with high sensitivity and selectivity. However, for studying the intra and inter-assay of the fabricated nanoflower like composite electrode, twelve fabricated working electrodes were taken and were immersed in 0.1 M PBS (pH 7.0) containing 0.1 μM concentration of DA. Eventually, their amperometric current response was recorded. The relative standard deviation observed for intra-and inter-assay was estimated at 2.3 and 2.6%, indicating that the fabrication protocol adapted for the construction of Ag-Cu@ZnO NFLC/GCE is stable and reliable. Adding to this, the stability of Ag-Cu@ZnO NFLC/GCE was also investigated by subjecting it to 1 μM concentration of DA for a period of 15 days. And the recorded amperometric current response was stable for this 15-day period of time. Furthermore, there was no substantial change in amperometric current response during the stability study of 15 days. These recorded observations indicate that the proposed sensor was stable. In this selectivity study, organic compounds and inorganic ions (0.02 mM of uric acid, ascorbic acid, caffeic acid, endorphin, phenethylamine, histamine, acetylcholine, serotonin, etc). They were used as potential interfering species capable of interrupting the amperometric signal response for DA. Hence, these results indicate that the proposed Ag-Cu@ZnO nanoflower like composite electrode can be used to monitor real-time sample analysis and another predominant factor is that the results do not exhibit any significant interference signals, compared to i-t current response of 0.1 μM DA

It indicates the excellent selectivity of the modified electrode towards DA.

However, the developed DA sensor in present work performance can be compared with other existing ZnO based DA sensors in **Table-1** whereas **Table-S1** shows the comparison of our present

View Article Online
DOI: 10.1039/D1MA00319D

Ag-Cu@ZnO nanoflower like composite DA sensor with other nanomaterial/composites sensors. The data for the tabular representation of recorded sensitivities was obtained from previously reported literature and the **Table-1** and **Table-S1** are evident that the fabricated electrode material may be used for magnificent sensing abilities with respect to better linear range and lowest limit of detection and high sensitivity in contrast to alternate modified electrodes. Perhaps this is associated with the excellent conductivity and enhanced surface area of fabricated electrode material. Apart from this, the material synthesis strategy involves a low cost and rapid single step synthesis strategy through which Ag-Cu@ZnO nanoflower like composites are obtained.

4. Conclusion

An Ag-Cu@ZnO nanoflower-like composite was produced using a simple low-cost fast single step synthesis process and drop cast on to GCE for DA electrochemical detection in this study. The Ag-Cu@ZnO-NFLC/GCE findings revealed a promising and improved electrochemical detection of DA, with excellent sensitivity and low detection limit. The Ag-Cu@ZnO-NFLC/GCE sensor showed a significant increase in oxidation peak currents, indicating that the as-prepared Ag-Cu@ZnO-NFLC/GCE sensor may be utilized as an electrochemical sensor for fast detection of DA. Furthermore, the Ag-Cu@ZnO-NFLC/GCE showed excellent stability, repeatability, and anti-interference properties. The Ag-Cu nanocomposite material provides enhanced support for the adsorption of DA and also helps in the mobility of the electrons between GCE and the analyte henceforth, enabling it to a remarkable increase in the electron transfer rate. When compared to GCE, Ag@ZnO, Cu@ZnO nanocomposite samples, the remarkable rise in redox peak currents on Ag-Cu@ZnO-NFLC/GCE with properly defined redox pair of dopamine enables it showing greater electrocatalytic activity. Overall, the synthesis technique used is simple and cost-effective,

View Article Online
DOI: 10.1039/D1MA00319D

making this sensor material ideal for the production of low-cost sensors with excellent stability and efficiency.

Declaration of competing Interest

The authors declare no competing of interest

Acknowledgements

Both authors Srikanth Ponnada and Dr. Annapurna Nowduri would like to acknowledge Andhra University College of Engineering-Visakhapatnam, India; Indian Institute of Science-Bangalore, India; IIT-Jodhpur, India and University grants commission-India for resource and technical support. Demudu Babu Gorle would like to acknowledge Indian Institute of Science-Bangalore, Andhra University college of Engineering-India University Grants Commission and Government of India for providing Dr. D. S. Kothari Postdoctoral Fellowship. Maryam Sadat Kiai would like to acknowledge Istanbul Technical University, Istanbul; Andhra University College of Engineering-Visakhapatnam, India. Saravanakumar Rajagopal would like to acknowledge Anna University-India; Andhra University College of Engineering-Visakhapatnam, India. All Authors would like to thank BioRender.com for **Fig.S3**.

View Article Online
DOI: 10.1039/D1MA00319D

References

[1] Wang, Z., Guo, H., Gui, R., Jin, H., Xia, J. and Zhang, F., **2018**. Simultaneous and selective measurement of dopamine and uric acid using glassy carbon electrodes modified with a complex of gold nanoparticles and multiwall carbon nanotubes. Sensors and Actuators B: Chemical, 255, pp.2069-2077.

[2] Pang, Y., Shi, Y., Pan, Y., Yang, Y., Long, Y. and Zheng, H., **2018**. Facile and sensitive detection of dopamine based on in situ formation of fluorescent polydopamine nanoparticles catalyzed by peroxidase-like ficin. Sensors and Actuators B: Chemical, 263, pp.177-182.

[3] Wang, A.J., Feng, J.J., Dong, W.J., Lu, Y.H., Li, Z.H. and Riekkola, M.L., **2010**. Spermine-graft-dextran non-covalent copolymer as coating material in separation of basic proteins and neurotransmitters by capillary electrophoresis. Journal of Chromatography A, 1217(31), pp.5130-5136.

[4] Gao, F., Liu, L., Cui, G., Xu, L., Wu, X., Kuang, H. and Xu, C., **2017**. Regioselective plasmonic nano-assemblies for bimodal sub-femtomolar dopamine detection. Nanoscale, 9(1), pp.223-229.

[5] Hubbard, K.E., Wells, A., Owens, T.S., Tagen, M., Fraga, C.H. and Stewart, C.F., **2010**. Determination of dopamine, serotonin, and their metabolites in pediatric cerebrospinal fluid by isocratic high performance liquid chromatography coupled with electrochemical detection. Biomedical Chromatography, 24, pp.626-631.

[6] Özcan, A., İlkbaş, S. and Özcan, A.A., **2017**. Development of a disposable and low-cost electrochemical sensor for dopamine detection based on poly (pyrrole-3-carboxylic acid)-modified electrochemically over-oxidized pencil graphite electrode. Talanta, 165, pp.489-495.

[7] Gupta, R., Rastogi, P.K., Ganesan, V., Yadav, D.K. and Sonkar, P.K., **2017**. Gold nanoparticles decorated mesoporous silica microspheres: a proficient electrochemical sensing scaffold for hydrazine and nitrobenzene. Sensors and Actuators B: Chemical, 239, pp.970-978.

View Article Online
DOI: 10.1039/D1MA00319D

[8] Wang, L., Zheng, Y., Lu, X., Li, Z., Sun, L. and Song, Y., **2014**. Dendritic copper-cobalt nanostructures/reduced graphene oxide-chitosan modified glassy carbon electrode for glucose sensing. Sensors and Actuators B: Chemical, 195, pp.1-7.

[9] Baghayeri, M., Veisi, H., Farhadi, S., Beitollahi, H. and Maleki, B., **2018**. Ag nanoparticles decorated Fe 3 O 4/chitosan nanocomposite: synthesis, characterization and application toward electrochemical sensing of hydrogen peroxide. Journal of the Iranian Chemical Society, 15(5), pp.1015-1022.

[10] Sharma, D., Sabela, M.I., Kanchi, S., Bisetty, K., Skelton, A.A. and Honarparvar, B., **2018**. Green synthesis, characterization and electrochemical sensing of silymarin by ZnO nanoparticles: experimental and DFT studies. Journal of Electroanalytical Chemistry, 808, pp.160-172.

[11] Lee, J., Farha, O.K., Roberts, J., Scheidt, K.A., Nguyen, S.T. and Hupp, J.T., **2009**. Metal–organic framework materials as catalysts. Chemical Society Reviews, 38(5), pp.1450-1459.

[12] Firooz, A.A., Ghalkhani, M., Albanese, J.A.F. and Ghanbari, M., **2020**. High electrochemical detection of dopamine based on Cu doped single phase hexagonally ZnO plates. Materials Today Communications, p.101716.

[13] Baig, N., Kawde, A.N. and Ibrahim, M., **2020**. Efficient ionic medium supported reduced graphene oxide-based sensor for selective sensing of dopamine. Materials Advances, 1(4), pp.783-793.

[14] Gao, F., Fan, T., Ou, S., Wu, J., Zhang, X., Luo, J., Li, N., Yao, Y., Mou, Y., Liao, X. and Geng, D., **2018**. Highly efficient electrochemical sensing platform for sensitive detection DNA methylation, and methyltransferase activity based on Ag NPs decorated carbon nanocubes. Biosensors and Bioelectronics, 99, pp.201-208.

[15] Dong, Y., Duan, C., Sheng, Q. and Zheng, J., **2019**. Preparation of Ag@zeolitic imidazolate framework-67 at room temperature for electrochemical sensing of hydrogen peroxide. Analyst, 144(2), pp.521-529.

[16] Qu, F., Lu, H., Yang, M. and Deng, C., **2011**. Electrochemical immunosensor based on electron transfer mediated by graphene oxide initiated silver enhancement. Biosensors and Bioelectronics, 26(12), pp.4810-4814.

View Article Online
DOI: 10.1039/D1MA00319D

[17] Drexler, S., Faria, J., Ruiz, M.P., Harwell, J.H. and Resasco, D.E., **2012**. Amphiphilic nanohybrid catalysts for reactions at the water/oil interface in subsurface reservoirs. Energy & fuels, 26(4), pp.2231-2241.

[18] Anaraki Firooz, A. and Keyhani, M., **2020**. The Effect of Different Dopants (Cr, Mn, ,Fe Photocatalytic on (Ni and Cu ,Co .Nanostructures ZnO of Properties International Journal of Nanoscience and Nanotechnology, 16(1), pp.59-65.

[19] Ahmad, R., Tripathy, N., Ahn, M.S., Bhat, K.S., Mahmoudi, T., Wang, Y., Yoo, J.Y., Kwon, D.W., Yang, H.Y. and Hahn, Y.B., **2017**. Highly efficient non-enzymatic glucose sensor based on CuO modified vertically-grown ZnO nanorods on electrode. Scientific reports, 7(1), pp.1-10.

[20] Khun, K., Ibupoto, Z.H., Liu, X., Mansor, N.A., Turner, A.P.F., Beni, V. and Willander, M., **2014**. An electrochemical dopamine sensor based on the ZnO/CuO nanohybrid structures. Journal of nanoscience and nanotechnology, 14(9), pp.6646-6652.

[21] Zhang, X., Zhang, Y.C. and Ma, L.X., **2016**. One-pot facile fabrication of graphene-zinc oxide composite and its enhanced sensitivity for simultaneous electrochemical detection of ascorbic acid, dopamine and uric acid. Sensors and Actuators B: Chemical, 227, pp.488-496.

[22] Lin, J., Huang, B., Dai, Y., Wei, J. and Chen, Y., **2018**. Chiral ZnO nanoparticles for detection of dopamine. Materials Science and Engineering: C, 93, pp.739-745.

[23] Song, Y., Han, J., Xu, L., Miao, L., Peng, C. and Wang, L., **2019**. A dopamine-imprinted chitosan Film/Porous ZnO NPs@ carbon Nanospheres/Macroporous carbon for electrochemical sensing dopamine. Sensors and Actuators B: Chemical, 298, p.126949.

[24] Yang, C., Zhang, C., Huang, T., Dong, X. and Hua, L., **2019**. Ultra-long ZnO/carbon nanofiber as free-standing electrochemical sensor for dopamine in the presence of uric acid. Journal of Materials Science, 54(24), pp.14897-14904.

[25] Zhao, M., Li, Z., Zhang, X., Yu, J., Ding, Y., Li, H. and Ma, Y., **2020**. Employing the interfacial barrier of P-rGO/ZnO microspheres for improving the electrochemical sensing performance to dopamine. Sensors and Actuators B: Chemical, 309, p.127757.

[26] Firooz, A.A., Ghalkhani, M., Albanese, J.A.F. and Ghanbari, M., **2020**. High electrochemical detection of dopamine based on Cu doped single phase hexagonally ZnO plates. Materials Today Communications, p.101716.

View Article Online
DOI: 10.1039/D1MA00319D

[27] Yue, H.Y., Zhang, H.J., Huang, S., Lu, X.X., Gao, X., Song, S.S., Wang, Z., Wang, W.Q. and Guan, E.H., **2020**. Highly sensitive and selective dopamine biosensor using Au nanoparticles-ZnO nanocone arrays/graphene foam electrode. Materials Science and Engineering: C, 108, p.110490.

[28] Zhihua, L., Xue, Z., Xiaowei, H., Xiaobo, Z., Jiyong, S., Yiwei, X., Xuetao, H., Yue, S. and Xiaodong, Z., **2021**. Hypha-templated synthesis of carbon/ZnO microfiber for dopamine sensing in pork. Food Chemistry, 335, p.127646.

[29] Kogularasu, S., Akilarasan, M., Chen, S.M., Chen, T.W. and Lou, B.S., **2019**. Urea-based morphological engineering of ZnO; for the biosensing enhancement towards dopamine and uric acid in food and biological samples. Materials Chemistry and Physics, 227, pp.5-11.

[30] Zhang, X. and Zheng, J., **2019**. Hollow carbon sphere supported Ag nanoparticles for promoting electrocatalytic performance of dopamine sensing. Sensors and Actuators B: Chemical, 290, pp.648-655.

[31] Li, Y.Y., Kang, P., Wang, S.Q., Liu, Z.G., Li, Y.X. and Guo, Z., **2021**. Ag nanoparticles anchored onto porous CuO nanobelts for the ultrasensitive electrochemical detection of dopamine in human serum. Sensors and Actuators B: Chemical, 327, p.128878.

[32] Zhang, C., Cao, Z., Zhang, G., Yan, Y., Yang, X., Chang, J., Song, Y., Jia, Y., Pan, P., Mi, W. and Yang, Z., **2020**. An electrochemical sensor based on plasma-treated zinc oxide nanoflowers for the simultaneous detection of dopamine and diclofenac sodium. Microchemical Journal, 158, p.105237.

[33] Ghosh, S., Das, R., Chowdhury, I.H., Bhanja, P. and Naskar, M.K., **2015**. Rapid template-free synthesis of an air-stable hierarchical copper nanoassembly and its use as a reusable catalyst for 4-nitrophenol reduction. RSC advances, 5(123), pp.101519-101524.

[34] Niu, H. Y., Liu, S. L., Cai, Y. Q., Wu, F. C. & Zhao, X. L. MOF derived porous carbon supported Cu/Cu2O composite as high performance non-noble catalyst. Microporous Mesoporous Mater. 219, 48–53 **(2016).**

[35] Najdovski, I., Selvakannan, P.R. and O'Mullane, A.P., **2014**. Electrochemical formation of Cu/Ag surfaces and their applicability as heterogeneous catalysts. *Rsc Advances*, *4*(14), pp.7207-7215.

[36] Konsolakis, M., Carabineiro, S.A.C., Papista, E., Marnellos, G.E., Tavares, P.B., Moreira, J.A., Romaguera-Barcelay, Y. and Figueiredo, J.L., **2015**. Effect of preparation

View Article Online
DOI: 10.1039/D1MA00319D

method on the solid state properties and the deN(2)O performance of CuO–CeO 2 oxides. Catalysis Science & Technology, 5(7), pp.3714-3727.

[37] García-Miranda Ferrari, A., Foster, C.W., Kelly, P.J., Brownson, D.A. and Banks, C.E., **2018**. Determination of the electrochemical area of screen-printed electrochemical sensing platforms. Biosensors, 8(2), p.53.

[38] Firooz, A.A., Ghalkhani, M., Albanese, J.A.F. and Ghanbari, M., **2021**. High electrochemical detection of dopamine based on Cu doped single phase hexagonally ZnO plates. Materials Today Communications, 26, p.101716.

[39] Yue, H.Y., Zhang, H.J., Huang, S., Lu, X.X., Gao, X., Song, S.S., Wang, Z., Wang, W.Q. and Guan, E.H., **2020**. Highly sensitive and selective dopamine biosensor using Au nanoparticles-ZnO nanocone arrays/graphene foam electrode. Materials Science and Engineering: C, 108, p.110490.

[40] Gorle, D.B. and Kulandainathan, M.A., **2016**. Electrochemical sensing of dopamine at the surface of a dopamine grafted graphene oxide/poly (methylene blue) composite modified electrode. RSC advances, 6(24), pp.19982-19991.

[41] Nagaraju, G., Prashanth, S.A., Shastri, M., Yathish, K.V., Anupama, C. and Rangappa, D., **2017**. Electrochemical heavy metal detection, photocatalytic, photoluminescence, biodiesel production and antibacterial activities of Ag–ZnO nanomaterial. Materials Research Bulletin, 94, pp.54-63.

[42] Lefatshe, K., Muiva, C.M. and Kebaabetswe, L.P., **2017**. Extraction of nanocellulose and in-situ casting of ZnO/cellulose nanocomposite with enhanced photocatalytic and antibacterial activity. Carbohydrate polymers, 164, pp.301-308.

[43] Kumar, K.A., Lakshminarayana, B., Suryakala, D. and Subrahmanyam, C., **2020**. Reduced graphene oxide supported ZnO quantum dots for visible light-induced simultaneous removal of tetracycline and hexavalent chromium. RSC Advances, *10*(35), pp.20494-20503.

[44] Muhammad, W., Ullah, N., Haroon, M. and Abbasi, B.H., **2019**. Optical, morphological and biological analysis of zinc oxide nanoparticles (ZnO NPs) using Papaver somniferum L. RSC advances, *9*(51), pp.29541-29548.

View Article Online
DOI: 10.1039/D1MA00319D

[45] Baig, N., Kammakakam, I. and Falath, W., **2021**. Nanomaterials: a review of synthesis methods, properties, recent progress, and challenges. Materials Advances, 2(6), pp.1821-1871.

[46] Ingavale, S., Marbaniang, P., Kakade, B. and Swami, A., **2021**. Starbon with Zn-N and Zn-O active sites: An efficient electrocatalyst for oxygen reduction reaction in energy conversion devices. Catalysis Today, 370, pp.55-65.

View Article Online
DOI: 10.1039/D1MA00319D

Figures

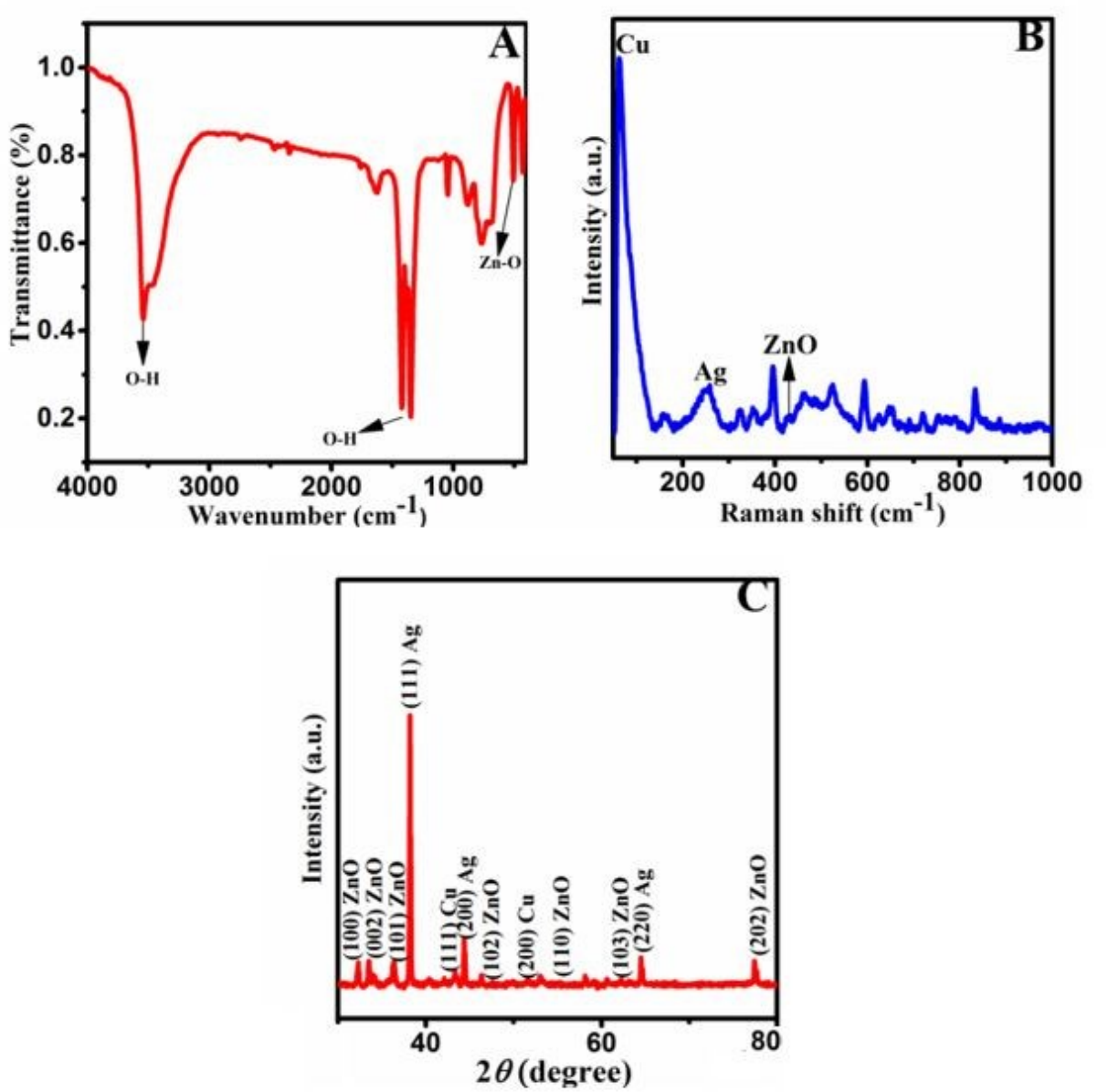

Fig. 1. **(A)** FTIR spectrum, **(B)** Raman spectrum, **(C)** XRD pattern

View Article Online
DOI: 10.1039/D1MA00319D

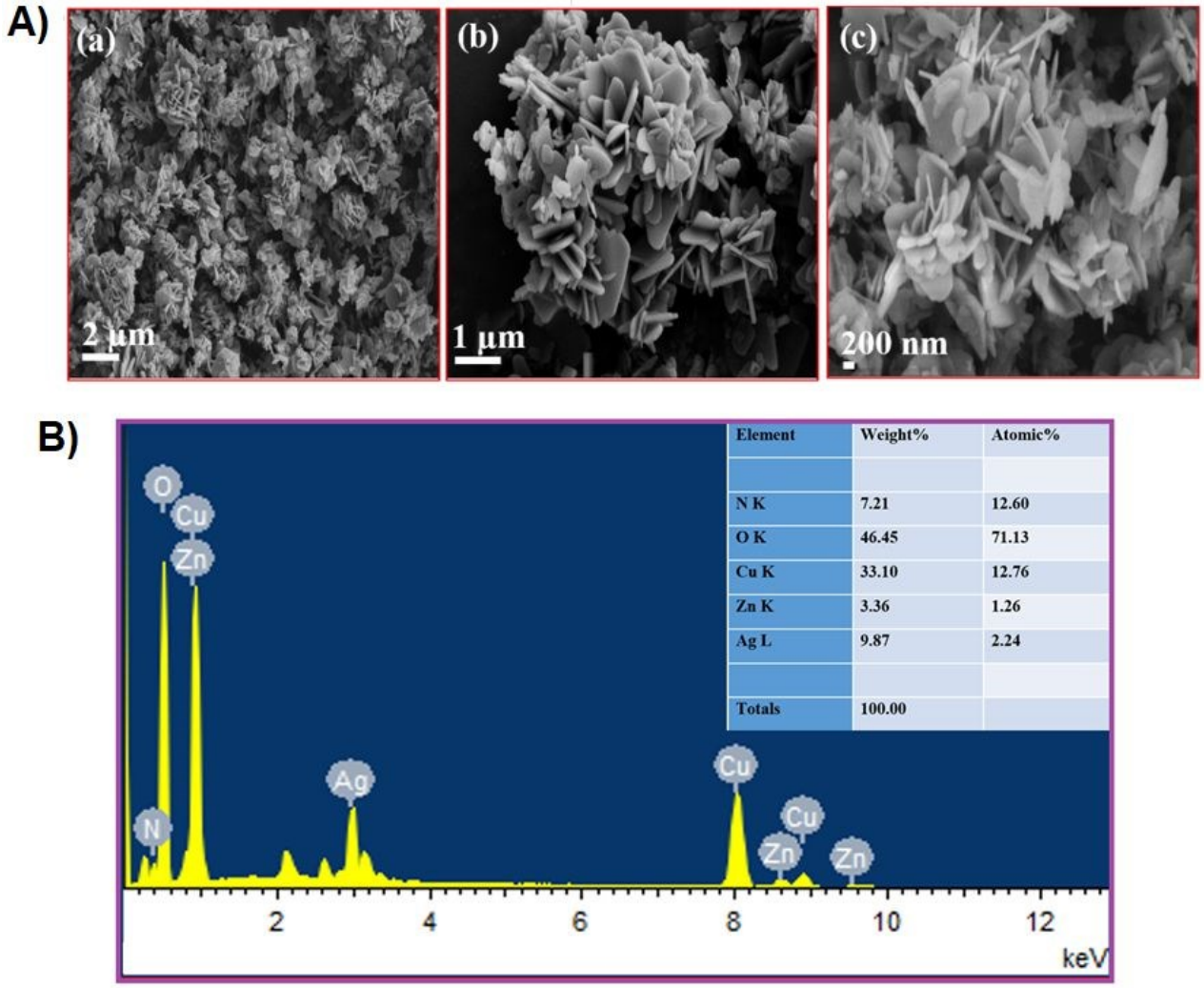

Fig. 2. **A)** SEM images of Ag-Cu@ZnO NFLC. **B)** EDX Spectra of Ag-Cu decorated ZnO-NFLC material; the inset is EDX Wt% of Ag-Cu decorated ZnO-NFLC material

View Article Online
DOI: 10.1039/D1MA00319D

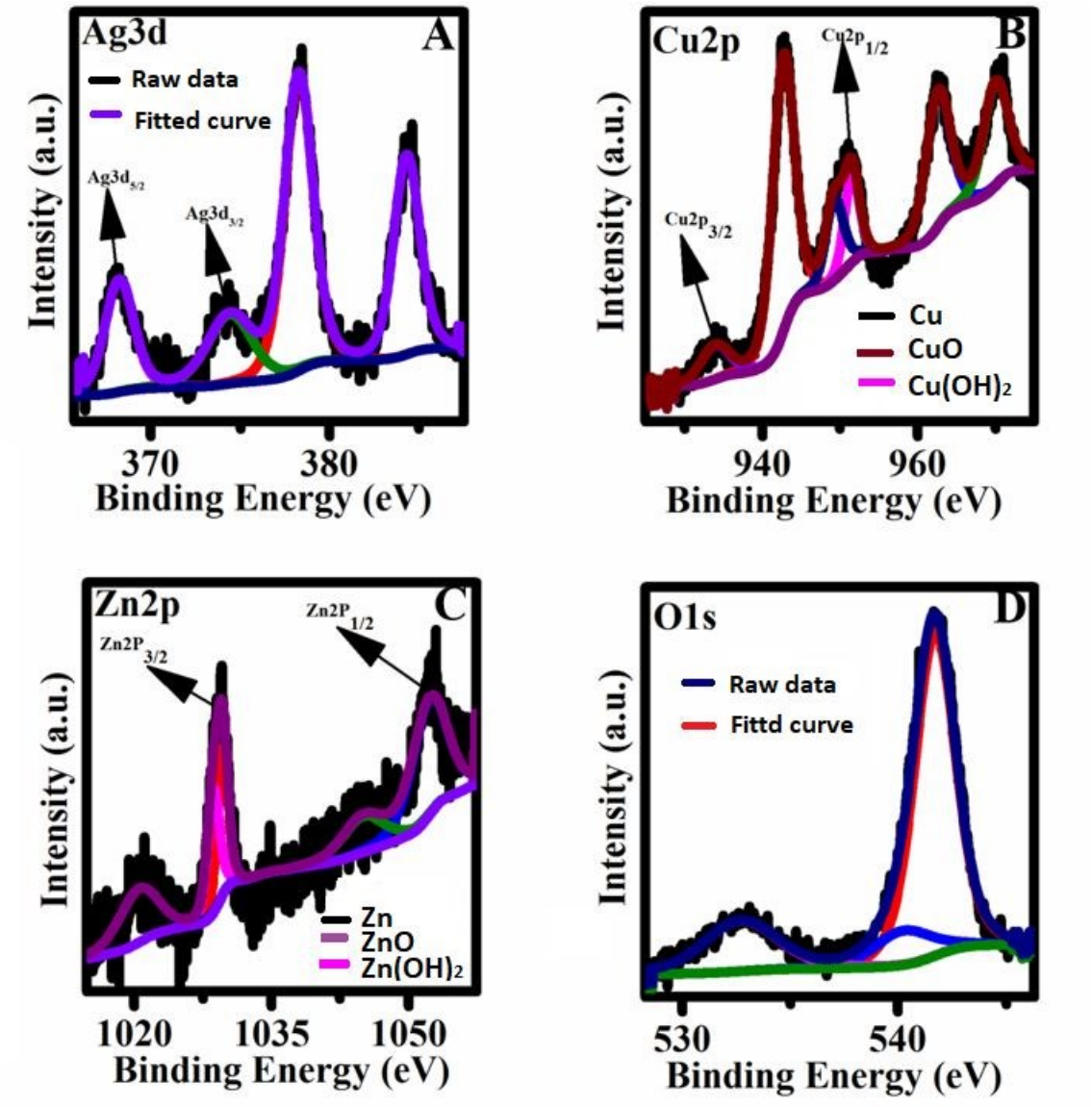

Fig. 3. XPS spectra of **(A)** Ag3d, **(B)** Cu2p, **(C)** Zn2p, and **(D)** O1s.

View Article Online
DOI: 10.1039/D1MA00319D

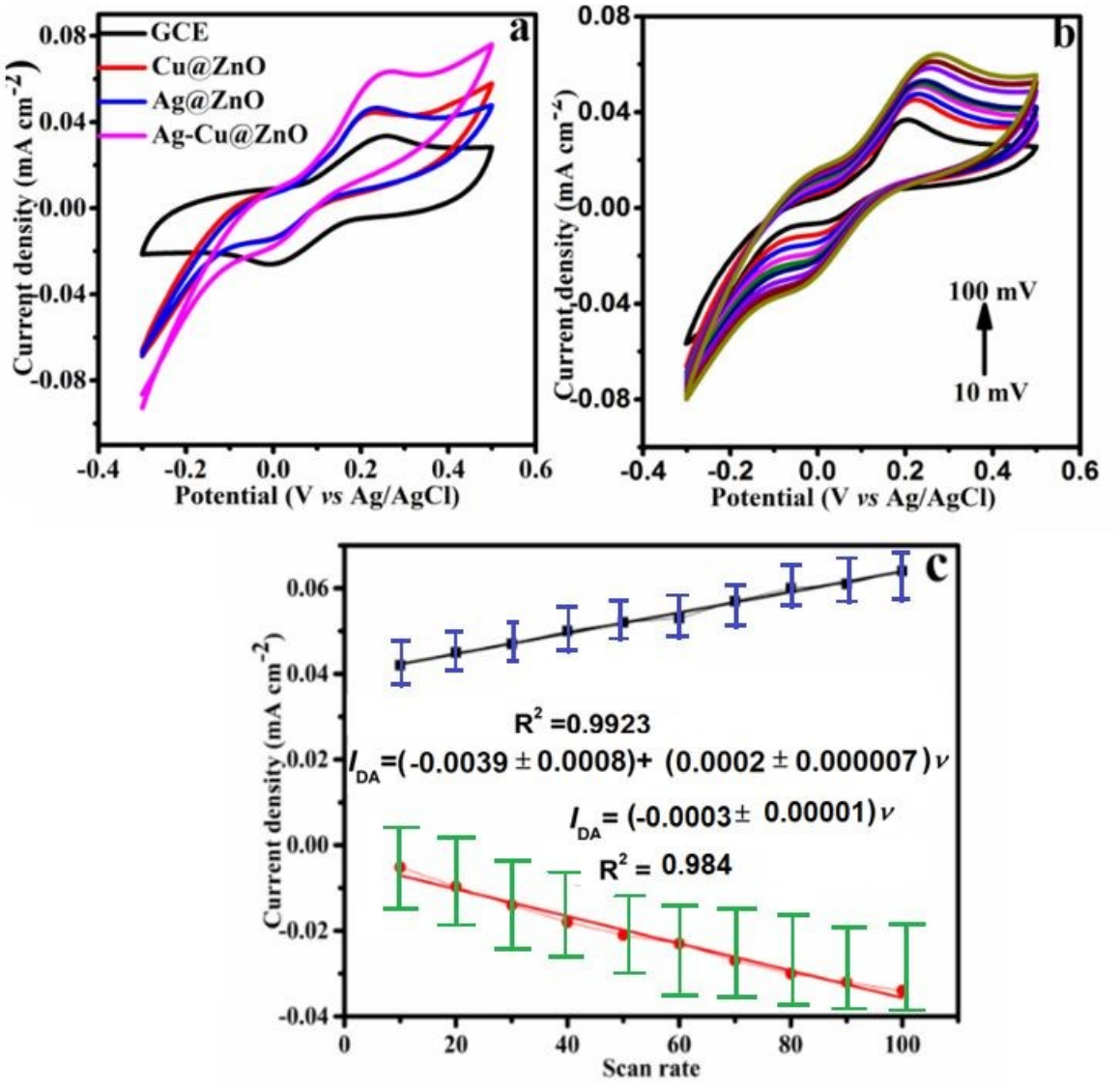

Fig. 4. (a) Cyclic voltagrams of bare GCE, Cu@ZnO, Ag@ZnO and Ag-Cu@ZnO NFLC modified GCE in 0.1M PBS (pH= 7.0) with 100 µM DA. Scan rate: 50 mV/s. **(b)** Cyclic voltamograms of 100µM DA on the Ag-Cu@ZnO modified GCE at different scan rates in 0.1 M PBS (pH=7.0). **(c)** Plot of the redox peak current versus the scan rate.

View Article Online
DOI: 10.1039/D1MA00319D

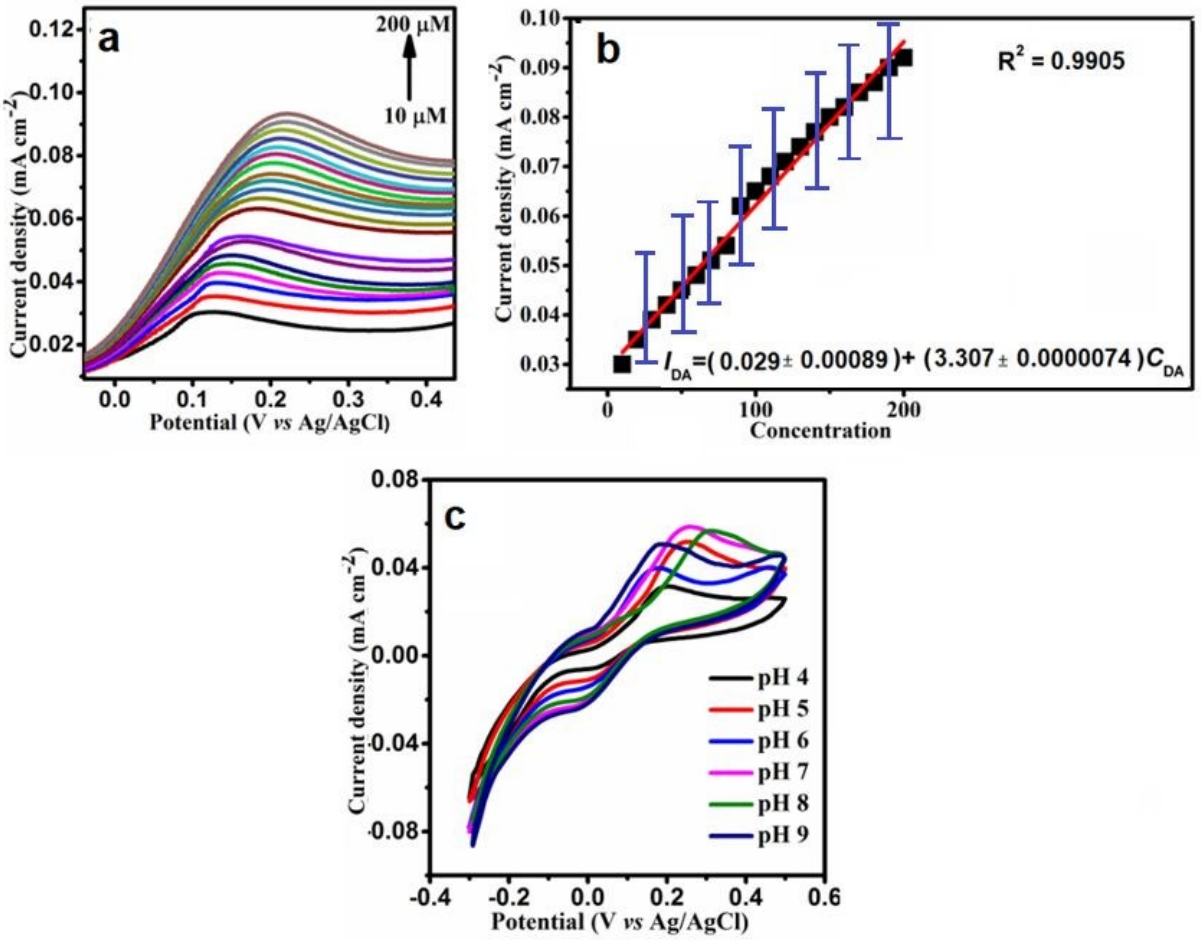

Fig. 5. (a) Differential pulse voltammetry curves of an Ag-Cu@ZnO NFLC modified GCE in 0.1 M PBS (pH=7.0) containing 10-200 µM DA. **(b)** The corresponding plot of the oxidation peak current of DA vs. DA concentration for the differential pulse voltammetry measurements. **(c)** Cyclic Voltagrams of Ag-Cu@ZnO NFLC modified GCE in 0.1 M PBS with different pH values containing 100 µM DA at scan rate of 50 mV/s.

View Article Online
DOI: 10.1039/D1MA00319D

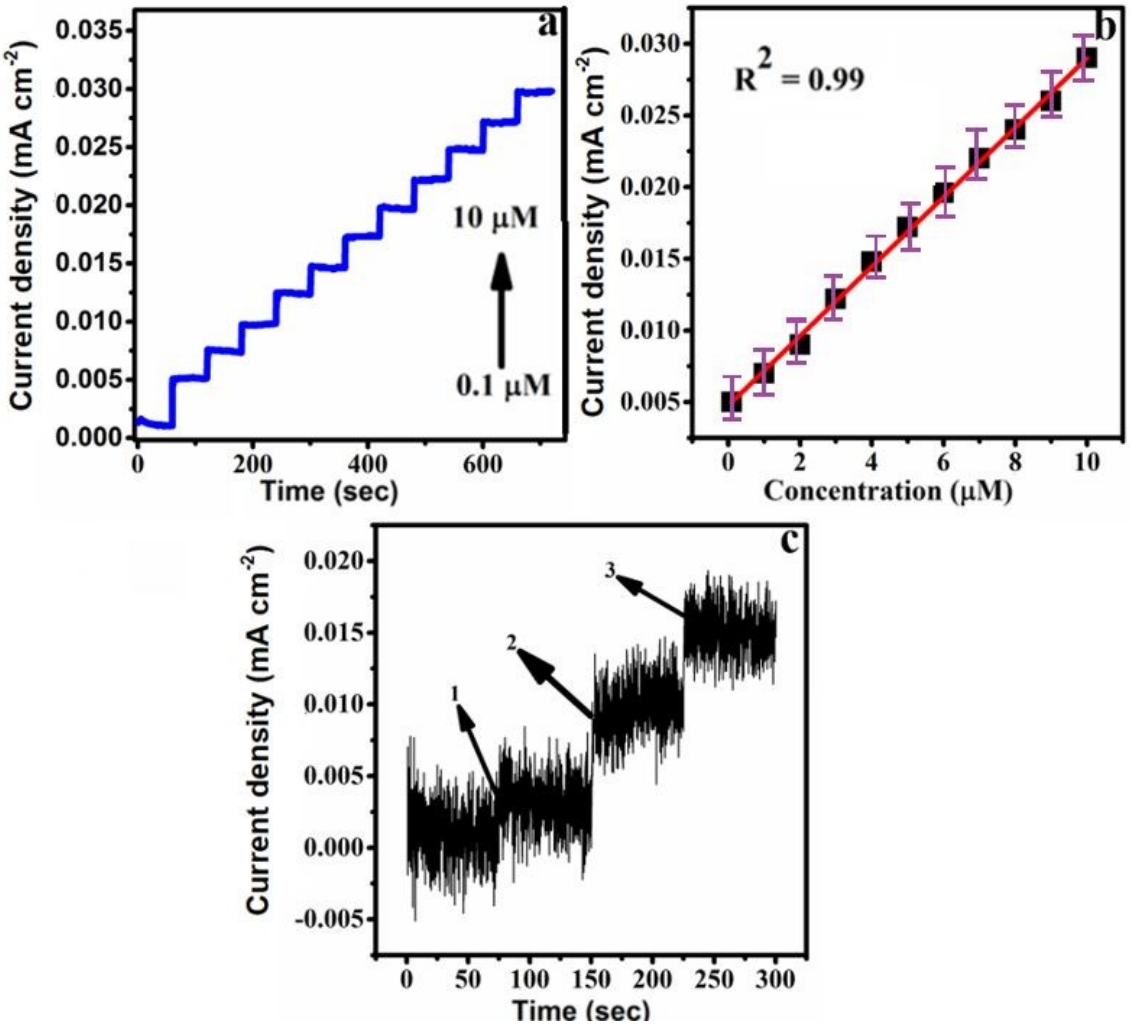

Fig. 6. **(a)** Typical amperometric curve obtained for Ag-Cu@ZnO modified GCE in 0.1M PBS (pH=7.0) at 0.24 V. **(b)** The corresponding calibration plot with the concentration of DA varying between 0.1-10 µM. **(c)** Amperometric response of an Ag-Cu@ZnO NFLC modified GCE after the subsequent addition of (1) 0.030, (2) 0.052, (3) 0.070 µM of DA in the presence of 1 µM of Urine sample.

View Article Online
DOI: 10.1039/D1MA00319D

Table-1 Comparison of ZnO based electrode materials for electrochemical sensing of dopamine

S. No.	Electrode/Nanomaterials	Analyte	LOD (μM) (S/N=3)	Sensitivity ($\mu AmM^{-1}cm^{-2}$)	Linear Range (μM)	Detection Method	Ref.
1	ZnO/CuO Nanohybrid structures	Dopamine	1.0×10^{-3} and 8.0	90.9	1.0×10^{-3}–8.0 μM	CV	**19**
2	rGO–ZnO/GCE	Dopamine	0.33	-	1–70 μM	DPV	**20**
3	Chiral ZnO nanoparticles-L cysteine.	Dopamine	0.791	-	-	-	**21**
4	DA-imprinted CS film/ZnO NPs @C/3D-KSC	Dopamine	0.39	757	0.12 nM-152 μM	CV	**22**
5	ZnO nanofibers/carbon fibers	Dopamine	0.402	-	6–20 μM	DPV	**23**
6	P-rGO/ZnO microspheres	Dopamine	-	1240.74	1-600 μM	SWV	**24**
7	Cu doped ZnO (Cu/ZnO)	Dopamine	0.055		0.1–20 μM	DPV, CV	**38**
8	Au-ZnO NCAs/GF	Dopamine	0.04	6.23	0-80 μM	CV	**39**
9	**Ag-Cu Decorated/ZnO Nanoflower like composite**	**Dopamine**	**0.21**	**0.68**	**0.1-10 μM**	**Amperometry**	**This work**